1662–1670 *Nucleic Acids Research, 2005, Vol. 33, No. 5*
doi:10.1093/nar/gki310

Single-stranded DNA-binding protein of *Deinococcus radiodurans*: a biophysical characterization

Gregor Witte, Claus Urbanke and Ute Curth*

Department of Biophysical Chemistry, Medical School Hannover, Hannover, Germany

Received January 28, 2005; Revised and Accepted February 28, 2005 DDBJ/EMBL/GenBank accession no. AJ564860

ABSTRACT

The highly conserved bacterial single-stranded DNA-binding (SSB) proteins play an important role in DNA replication, repair and recombination and are essential for the survival of the cell. They are functional as tetramers, in which four OB(oligonucleotide/oligosaccharide binding)-folds act as DNA-binding domains. The protomer of the SSB protein from the extremely radiation-resistant organism *Deinococcus radiodurans* (*Dra*SSB) has twice the size of the other bacterial SSB proteins and contains two OB-folds. Using analytical ultracentrifugation, we could show that *Dra*SSB forms globular dimers with some protrusions. These *Dra*SSB dimers can interact with two molecules of *E.coli* DNA polymerase III χ subunit. In fluorescence titrations with poly(dT) *Dra*SSB bound 47–54 nt depending on the salt concentration, and fluorescence was quenched by more than 75%. A distinct low salt binding mode as for *Eco*SSB was not observed for *Dra*SSB. Nucleic acid binding affinity, rate constant and association mechanism are quite similar for *Eco*SSB and *Dra*SSB. In a complementation assay in *E.coli*, *Dra*SSB took over the *in vivo* function of *Eco*SSB. With *Dra*SSB behaving almost identical to *Eco*SSB the question remains open as to why dimeric SSB proteins have evolved in the *Thermus* group of bacteria.

INTRODUCTION

Single-stranded DNA-binding (SSB) proteins play a vital role in the sustainment of almost every form of life we know on earth. They protect and configure the vulnerable state of unwound and single-stranded DNA (ssDNA) for efficient use by enzymes involved in DNA metabolism, such as replication, recombination and repair. The function of ssDNA binding is found in seemingly very different protein classes ranging from monomers over homodimers and homotetramers to heterooligomers. However, all SSB proteins share a structural motif called OB(oligonucleotide/oligosaccharide binding)-fold (1,2). One of these classes is formed by homotetrameric SSB proteins which play a vital role in bacteria and eukaryotic mitochondria. Their 3D structures, which have been determined for such divergent organisms as *E.coli* and human, are quite similar (3–5), and thus this class of proteins constitutes an evolutionary strictly conserved structural principle.

In light of this structural conservation, it was surprising when *in silico* analysis of the *ssb* genes from the bacterial *Thermus* group suggested the proteins encoded by these genes to belong to the class of homotetrameric SSBs, although they were about twice the size compared with other proteins of this class. The protomers of *Thermus* SSBs contain two OB-folds per monomer, and therefore it was not surprising that these proteins form homodimers (6). These homodimers thus mimic the homotetrameric SSBs.

One might argue that the origin of homodimeric SSB proteins was a duplication of the gene of the homotetrameric SSB proteins, and there have been some speculations about evolutionary *raison d'être* for such a duplication. One of these speculations puts an evolutionary advantage to the fact that the two OB-folds in the homodimeric SSB can evolve separately and thus can help in surviving the hostile environments *Thermus* bacteria live in (7).

Recently, several homodimeric SSBs from different *Thermus* species have been cloned and isolated as proteins (8,9) and for the SSB from *Deinococcus radiodurans* (*Dra*SSB) a 3D structure has been determined by X-ray crystallography (7). The overall structure of *Dra*SSB in its OB-folds is quite similar to the human mitochondrial and *E.coli* SSB structure.

However, owing to the lack of solid biochemical and biophysical data on the solution properties of *Dra*SSB, the interpretation of structural details remains speculative. We, therefore, have isolated the gene for this protein, expressed it in *E.coli* and purified it to homogeneity. In this work, we will describe the biophysical and biochemical characterization of

*To whom correspondence should be addressed at Medizinische Hochschule Hannover, Zentrale Einrichtung für biophysikalisch-biochemische Verfahren, Carl-Neuberg-Strasse 1, D-30625 Hannover, Germany. Tel: +49 511 532 3707; Fax: +49 511 532 5966; Email: curth.ute@mh-hannover.de

the protein itself and its protein–protein and protein–DNA interactions. As in the structure, the overall properties of *Dra*SSB resemble those of the homotetrameric SSBs albeit with some differences in detail.

MATERIALS AND METHODS

Buffers and reagents

D.radiodurans R_1 strain DSM20539 was purchased from Deutsche Sammlung von Mikroorganismen und Zellkulturen (Germany). Poly(dT) (~1400 nt in length), poly(rU) and poly(dA–dT) were purchased from Amersham Biosciences. Polynucleotide concentrations are given in monomer residues throughout the text and were determined spectrophotometrically using absorption coefficients of 8600 M^{-1} cm^{-1} for poly(dT) at maximum (10) and 9200 M^{-1} cm^{-1} and 6700 M^{-1} cm^{-1} at 260 nm for poly(rU) and poly(dA–dT), respectively (11).

Protein concentrations were determined using the absorption coefficients at 280 nm calculated from amino acid composition (12): 29 400 M^{-1} cm^{-1} for χ subunit of *E.coli* DNA polymerase III, 82 000 M^{-1} cm^{-1} for *Dra*SSB dimer and 113 000 M^{-1} cm^{-1} for *Eco*SSB tetramer. *Dra*SSB and *Eco*SSB concentrations are given in dimers and tetramers, respectively, throughout the text.

All experiments were carried out in potassium phosphate buffer at pH 7.4 (KP_i) containing NaCl as neutral salt. Concentrations are given at the respective experiments.

Cloning of *D.radiodurans ssb* gene

The *ssb* gene was amplified from heat disrupted *D.radiodurans* cells by PCR. Primers used were 5′-GGAGACC*ATGGCCC-GAGGCATGAACCA*-3′ for forward and 5′-GAAGAGGAT-CC*TCATGTTGGGTGTCCTTGGTG*-3′ for reverse priming. Primers were selected to include start and stop codon containing sequences (italic) of the *Dra*SSB gene accession no. AJ564860 (*vide infra*). PCR was carried out using *Pfu* DNA polymerase (Stratagene), 200 μM dNTP and 0.5 μM of each primer with an annealing temperature of 53°C and 30 cycles. The PCR product was purified using a PCR purification kit (Qiagen). The amplified product was digested with NcoI and BamHI and cloned into the NcoI and BamHI sites of pET15b (Novagen) to generate pET15b-*Dra*SSB. This plasmid was used to transform the *E.coli* strain LK111λ. The procedure was repeated using a different lot of the *D.radiodurans* strain DSM20539. Different clones were selected and the *Dra*SSB gene was completely sequenced in both strands (MWG Biotech) for both lots of *D.radiodurans* used without finding any differences.

Expression and purification of SSB protein from *D.radiodurans*

For protein expression, the plasmid pET15b-*Dra*SSB was used to transform the *E.coli* strain BL21(DE3) pLysS. A volume of 900 ml of an overnight culture grown in the presence of 100 μg/ml ampicillin and 30 μg/ml chloramphenicol at 30°C was used to inoculate 10 l of standard Luria–Bertani (LB) medium and the cells were grown at 30°C. An aliquot of 100 ml of the overnight culture was used for plasmid preparation (Qiagen) and subsequent DNA sequencing to confirm the sequence of the expressed gene shortly before induction. Protein expression was induced after growing the cells to $A_{600\ nm} = 1.0$ by the addition of 1 mM isopropyl-β-D-thiogalactopyranoside and was continued for 4 h. After cell harvesting and washing with buffer W [0.2 M NaCl, 50 mM Tris–HCl, pH 8.3, 1 mM EDTA and 10% (w/v) sucrose], the pellet was resuspended in buffer S (buffer W containing 15 mM spermidin), frozen and stored at −70°C.

When cells were thawed, one tablet of 'complete EDTA-free' protease inhibitor (Roche) per 50 ml and 0.04% sodium-desoxycholat were added. After sonification and removing of cell debris by preparative ultracentrifugation, proteins were precipitated by the addition of polyethylenimine, pH 6.9 (final concentration 0.4%) for 20 min at 4°C and pelleted. The pellet was extracted with TGE400 buffer [0.4 M NaCl, 50 mM Tris–HCl, pH 8.3, 1 mM EDTA and 20% (v/v) glycerol] and insoluble material was removed by centrifugation. The clear supernatant was precipitated with 20% (w/v) $(NH_4)_2SO_4$ overnight at 4°C. The pellet was redissolved in TGE400 and loaded on a BlueSepharose column (13) equilibrated in the same buffer. After washing the column with TGE400, a linear salt gradient (0.4–3 M NaCl in the same buffer) was used to elute the protein. Fractions were analyzed by SDS–PAGE (14), pooled and precipitated with 20% (w/v) $(NH_4)_2SO_4$. The pellet was redissolved in SBP buffer [0.5 M NaCl, 20 mM KP_i, pH 7.4, 1 mM EDTA and 20% (v/v) glycerol] and dialyzed against the same buffer containing 1 M NaCl and 60% (v/v) glycerol and stored at −20°C. The protein preparation was at least 97% pure as judged from Coomassie Brillant Blue stained SDS gel.

Complementation assay

In *E.coli* strain RDP268, the chromosomal SSB gene is replaced by a kanamycin resistance and the essential SSB protein is encoded by the plasmid pACYCssb (15). This plasmid confers chloramphenicol resistance to the cells. pACYCssb is essential for the survival of the cells and can be replaced by another plasmid, only if it contains a gene whose product can take over *Eco*SSB function *in vivo*. We used the strain RDP268 to transform the pSF1 (16) derivative pSF1-*Dra*SSB, which carries the *Dra*SSB gene under the control of the λ p_L promotor and confers ampicillin resistance. In RDP268 (pSF1-*Dra*SSB), the p_L promotor is not repressed leading to a high constitutive *Dra*SSB expression. The cells were grown in the presence of 100 μg/ml ampicillin and 5 μg/ml kanamycin but omitting chloramphenicol. After four subsequent inoculations of 4 ml LB medium, allowing the cells to grow for 24 h at 37°C, 100–200 cells were plated on LB medium containing 100 μg/ml ampicillin and 5 μg/ml kanamycin. Clones that lost the plasmid pACYCssb were identified by replica plating on LB medium containing 30 μg/ml chloramphenicol and 5 μg/ml kanamycin. SSB proteins in chloramphenicol-sensitive clones were characterized by western blot analysis.

Western blot analysis

SSB proteins blotted onto a PVDF membrane were detected immunologically by a polyclonal anti-*Eco*SSB serum from rabbit. Rabbit antibodies were marked by alkaline phosphatase-conjugated goat anti-rabbit antibodies and detected by alkaline

phosphatase chemiluminescence reaction (CDP-Star, Tropix). Exposed X-ray films were digitized.

Analytical ultracentrifugation

Analytical ultracentrifugation was performed in a Beckman XL-A analytical ultracentrifuge using an An50Ti or An60Ti rotor at 20°C. Concentration profiles were measured with UV absorption scanning optics of the centrifuge.

Sedimentation velocity

Sedimentation velocity experiments were carried out in double-sector centerpieces at 20 000–60 000 r.p.m. Sedimentation rate constants were obtained by analyzing the movement of the sedimenting boundary or by fitting a numerical solution of Lamm's differential equation (17) to the concentration profiles using the BPCFIT software package (18). For analysis of interactions, data were evaluated with SEDFIT (19) to yield diffusion-corrected differential sedimentation coefficient distributions c(s). The areas under separate peaks of such a distribution are a measure of the absorption of the differently sedimenting components and can be analyzed to yield a binding isotherm (20). For hydrodynamic analysis, *s*-values were corrected to $s_{20°C,W}$. Since the partial specific volume of complexes of different macromolecules with unknown stoichiometry cannot be calculated, such a correction could not be performed in these cases and uncorrected s-values had to be used.

Sedimentation equilibrium

Sedimentation equilibrium experiments for molar mass determination were carried out with 120 µl samples in 6-channel-centerpieces in an An50Ti rotor running at 20°C at 14 000 r.p.m. until no change in concentration distribution could be observed for at least 12 h. Scans from these 12 h were averaged and apparent molar masses were evaluated by fitting the concentration gradient with

$$A(x) = A_{\text{offset}} + A(x_0) \cdot e^{\frac{M(1-\bar{\nu}\rho)}{2RT}\omega^2\left(x^2-x_0^2\right)}$$

where x is the distance from centre of rotation, ω is the angular velocity of the rotor, $\bar{\nu}$ is the partial specific volume of the solute calculated from amino acid composition (21), ρ is the density of the solution, $A(x)$ is the absorption at position x, $A(x_0)$ is the absorption of the macromolecule at x_0 and A_{offset} is the absorption of the buffer measured near the meniscus after sedimenting the protein for 8 h at 44 000 r.p.m. Fitting was carried out with BPCFIT (18). Protein stability against denaturation by guanidine hydrochloride (GuaHCl) was measured in sedimentation equilibrium experiments using different concentrations of GuaHCl. Note that guanidinium denatured proteins have a molar mass somewhat higher than the molar mass of the covalent protein chain owing to preferential binding of the denaturant.

DNA melting curves

DNA melting curves were measured in a DMR10 (Zeiss, Germany) spectrophotometer as described previously (22) using a heating rate of 20 K/h. The experiments were carried out with 38 µM nucleotides of poly(dA–dT) in 75 mM NaCl, 20 mM KP_i. As long as the temperature did not exceed 50°C, no significant differences between heating and cooling curves could be observed, confirming the reversibility of melting. Above 50°C, irreversible heat denaturation of *Dra*SSB occurred.

Fluorescence titrations

Fluorescence titrations were carried out in a Schoeffel RRS1000 spectrofluorimeter as described previously (23). Excitation wavelength was 295 nm and emission was detected at 350 nm. To avoid inner filter effects, concentrations of protein and single-stranded nucleic acid were chosen such that the total absorption of the solution did not exceed 0.05 throughout the titration. After each addition, the solution was allowed to equilibrate between 60 and 600 s until no fluorescence change could be observed any longer. Binding curve analysis was carried out using the model of Schwarz and Watanabe (24) with n as binding site size, $\omega \cdot K$ as cooperative binding affinity and fluorescence quench Q_f as parameters. Fluorescence quench is defined as $1 - F_{\text{bound}}/F_{\text{free}}$, where F_{free} and F_{bound} denote the fluorescence intensities measured for free and nucleic acid bound protein, respectively.

Stopped-flow kinetics

Stopped flow kinetics for the determination of the association rate constant of *Dra*SSB and poly(dT) was measured with an Applied Photophysics π* system using tryptophan fluorescence excited at 295 nm and observed through a WG320 filter. Several traces collected for each concentration were accumulated to reduce noise. When analyzing the binding of SSB proteins to long ssDNA, a simple bimolecular model is insufficient, since one has to consider the length distribution of gaps between protein covered sites. At intermediate saturation, there will be gaps between bound proteins too short to accommodate binding of further ligands. A thermodynamic equilibrium model for such a binding of a multidentate ligand to a long linear polymer (24) has been extended to a kinetic model (10,25). In this model, it is assumed that in the rate-limiting bimolecular step of association, SSB forms an initial stable encounter complex with a shorter binding site length and subsequently redistributes in a monomolecular manner on the ssDNA. Data measured at different concentrations were analyzed by globally fitting the parameters of this kinetic model using the program BPCFIT (18).

RESULTS

Protein sequence

We amplified the postulated reading frame for *D.radiodurans* SSB protein from the strain DSM20539. Sequencing of the PCR product yielded an open reading frame (ORF) coding for 301 amino acids. The sequence was at variance with the genomic sequence published (EMBL accession no. AE001873, gene DR0099), which obviously contained sequencing errors leading to frameshifts and an early termination sequence. The same discrepancy was also found recently by others (9). The corrected *Dra*SSB sequence was deposited in the EMBL database [accession numbers AJ564860 (this paper) and AY293617 (9)]. The ORF shows a large sequence similarity to other SSB proteins, such as SSBs from *Thermus aquaticus*

and *Thermus thermophilus* (6,8,9). Comparing the *Dra*SSB sequence with other bacterial SSB sequences [e.g. from *E.coli* (26)] shows that the N-terminal DNA-binding domain (the OB-fold) occurs twice in tandem in *Dra*SSB and the other *Thermus* SSBs while it occurs only once in the *Eco*SSB gene. A possible explanation for this difference is a gene duplication event that occurred during the evolution of the *Thermus* group SSBs. The highly conserved acidic C-terminus with the consensus sequence DDDIPF is also present in *Dra*SSB (EDDLPF).

Structural characterization of *Dra*SSB

*Dra*SSB protein overexpressed in *E.coli* was purified to homogeneity (>97%). Figure 1 shows a sedimentation velocity experiment in the analytical ultracentrifuge. Analysis of the sedimenting boundary using Lamm's differential equation yields a sedimentation rate constant of $s_{20°C,W} = 3.95$S and a diffusion constant of $D_{20°C,W} = 6.3 \times 10^{-11}$ m^2 s^{-1}. Combining these two values with the partial specific volume of 7.23×10^{-4} m^3 kg^{-1} calculated from the amino acid composition (21) gives a molar mass of 55 kg/mol. The molar mass of the covalent protein chain of *Dra*SSB is calculated to be 32.7 kg/mol. Since the diffusion coefficient evaluated from the broadening of the sedimenting boundary tends to be overestimated owing to artificial broadening effects (27), a molar mass derived from sedimentation and diffusion coefficients constitutes a lower limit and the finding, thus, is a clear indication that the native state of *Dra*SSB is a homodimer. Using the molar mass of the dimer as calculated from the amino acid composition, the sedimentation rate constant of 3.95S leads to a frictional ratio of 1.5. Since for globular hydrated proteins this frictional ratio is expected to be 1.1–1.2 (27), a value of 1.5 shows the protein to be either strongly asymmetric or globular with several protuberances. For *Eco*SSB, it has been shown that the large frictional coefficient of 1.42 is reduced to 1.25 when cleaving off the C-terminal third of the protein (11). Thus, it seems likely that similar to *Eco*SSB the C-terminal part of *Dra*SSB extends into the solution. This is also supported by gel filtration experiments, which suggest *Dra*SSB to be asymmetric (9), and by recent X-ray crystallographic studies where the C-terminal part of *Dra*SSB could not be localized (7), probably owing to large disorder.

Sedimentation equilibrium in the analytical ultracentrifuge gave a molar mass of $M = 62 \pm 2$ kg/mol with no indication of multiple species or aggregation, confirming the result obtained for a differently prepared *Dra*SSB before (9) and clearly showing again that *Dra*SSB forms homodimers.

We have tested the conformational stability of *Dra*SSB by sedimentation equilibrium experiments in the presence of different concentrations of GuaHCl. GuaHCl denaturation, monitored by changes in the apparent molar mass (Figure 2), results in a transition midpoint at 1 M denaturant. *Dra*SSB, therefore, is clearly more sensitive to GuaHCl-induced denaturation than *Eco*SSB whose transition midpoint is at 1.7 M (Figure 2). Thus, the folded state of *Dra*SSB is less stable than the bacterial prototype *Eco*SSB. This relative instability is also reflected in the temperature stability of these two proteins. While DNA melting experiments with *Eco*SSB can be performed up to 65°C, *Dra*SSB irreversibly denatures at temperatures above 50°C.

In vivo detection of SSB in *D.radiodurans*

It remains to be demonstrated that the ORF cloned and expressed in *E.coli* encodes a genuine protein of *D.radiodurans*. Western blot analysis shows that a polyclonal anti-*Eco*SSB serum cross-reacts with cloned *Dra*SSB and detects a correctly sized protein in a total protein extract from *D.radiodurans* (Figure 3A).

*Dra*SSB can replace *Eco*SSB *in vivo*

Though different in oligomerization, *Eco*SSB and *Dra*SSB share the ssDNA-binding folds (OB-fold) (7) and the C-terminal region, for which important protein–protein interactions have been shown (28–30). Therefore, we tested whether *Dra*SSB can take over the *Eco*SSB function *in vivo* using an *ssb* deletion strain (RDP268). In RDP268, the chromosomal *ssb* gene has been replaced by a kanamycin resistance and the vital SSB function is supplied by *Eco*SSB encoded on the chloramphenicol resistance conferring plasmid pACYCssb (15). After transformation of these cells using pSF1-*Dra*SSB,

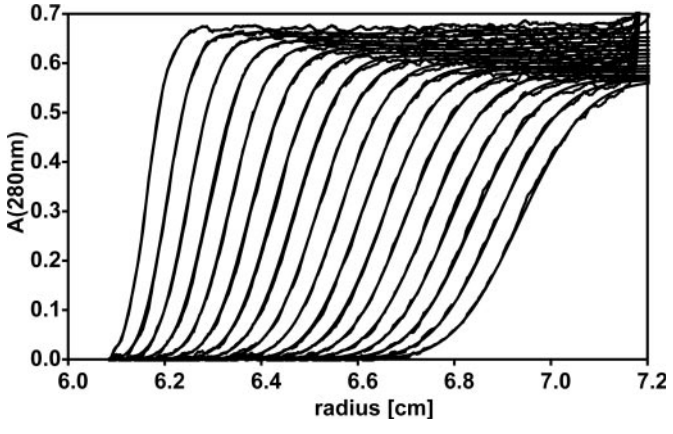

Figure 1. Sedimentation of *Dra*SSB in the analytical ultracentrifuge. A sample containing 7.5 μM *Dra*SSB in 0.3 M NaCl and 20 mM KP_i was centrifuged at 20°C and 60 000 r.p.m.; scans were taken every 8 min. Smooth lines correspond to theoretical traces for a sedimentation coefficient of $s_{20°C,W} = 3.95$S and a molar mass of 55 kg/mol ($D_{20°C,W} = 6.3 \times 10^{-11}$ m^2 s^{-1}) calculated with a numerically integrated Lamm differential equation (cf. Materials and Methods).

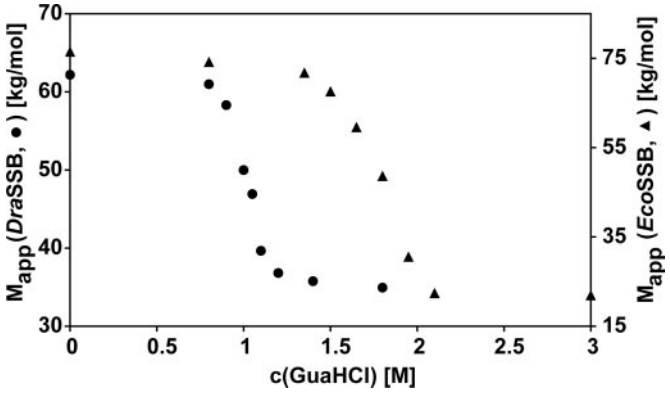

Figure 2. Guanidinium-induced unfolding of 4 μM *Dra*SSB (circles) and 3.5 μM *Eco*SSB (triangles) in 0.3 M NaCl and 20 mM KP_i. Apparent molar masses (cf. Materials and Methods) were determined from sedimentation equilibrium centrifugation at 20°C and 14 000 r.p.m. Note the different axes.

which encodes resistance against ampicillin, and subsequent inoculations (cf. Materials and Methods), we could isolate clones that showed resistance against ampicillin and kanamycin but not against chloramphenicol. These clones must have lost the pACYCssb plasmid encoding for *Eco*SSB. SSB expression was examined by western blot analysis using an anti-*Eco*SSB serum as a primary antibody (Figure 3B).While in RDP268 *Eco*SSB could be detected, the chloramphenicol-sensitive clones showed an expression of only *Dra*SSB (32.7 kDa) but not of *Eco*SSB (18.8 kDa).

*Dra*SSB binding to ssDNA

Whenever two macromolecules interact, the resulting complex will have a larger mass than any of the single components and, thus, it will sediment faster than the single species. Binding SSB proteins to polymeric ssDNA [poly(dT)] results in a dramatic increase in sedimentation rate. At 0.3 M NaCl, 20 mM KP_i poly(dT) of ~1400 nt in length has a sedimentation coefficient of 8S. Addition of different amounts of *Dra*SSB (3.6S) to this poly(dT) leads to an increase of this sedimentation coefficient up to 26S at saturation. Saturation point is reached at a stoichiometry of 50 ± 5 nt per *Dra*SSB dimer corresponding to a complex of ~28 SSB proteins on each poly(dT) strand (data not shown).

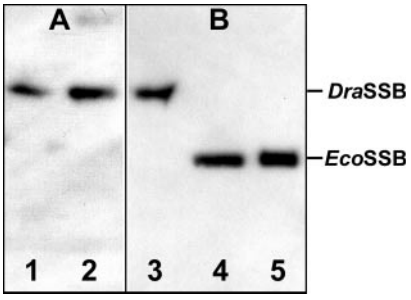

Figure 3. Verification of cloned *Dra*SSB as a genuine *D.radiodurans* protein (A) and complementation assay (B). Samples were boiled in 1% SDS sample buffer, proteins were separated in Tricin SDS–PAGE (40), blotted on PVDF membrane and immunologically detected with a polyclonal rabbit anti-*Eco*SSB serum. (**A**) Cell extract from *D.radiodurans* (lane 1) compared with 200 ng purified recombinant *Dra*SSB (lane 2). (**B**) Lane 3, RDP268 (pSF1-*Dra*SSB) cells express only *Dra*SSB; lane 4, RDP268 (pACYCssb) cells express only *Eco*SSB; and lane 5, purified recombinant *Eco*SSB (15 ng). Lane 3 and lane 4 contain equal amounts of cells.

All homotetrameric SSB proteins studied so far show a dramatic decrease of tryptophan fluorescence when binding to ssDNA (25,31,32). Figure 4 shows titrations of *Dra*SSB with poly(dT) at high salt (0.3 M NaCl and 20 mM KP_i) and low salt (1 mM NaCl and 1 mM KP_i) conditions. For comparison, similar titrations of *Eco*SSB are shown. Under high salt conditions, binding isotherms give a stoichiometry of 54 ± 2 nt/*Dra*SSB(dimer) and tryptophan fluorescence is quenched by 87 ± 2%. At low salt conditions, the stoichiometry is reduced to 47 ± 2 nt/*Dra*SSB(dimer) and the fluorescence quench is diminished to 77 ± 2%. In both the cases, the cooperative affinity is estimated to be in the range of 10^7–10^8 M^{-1}.

Stopped-flow analysis of the association of *Dra*SSB to poly(dT) at high salt (0.3 M NaCl and 20 mM KP_i) (Figure 5) is compatible with a binding mechanism where the initial binding of the protein uses a short stretch of nucleotides that are bound in a bimolecular mechanism with an association rate constant of 2.1×10^8 M^{-1} s^{-1}. Subsequently, the protein–nucleic acid complex rearranges in a monomolecular reaction to reach its final binding site size (cf. Materials and Methods). The association mechanism and rate constant are in accordance with the other homotetrameric SSB proteins investigated so far (10,25).

Since binding of SSB to poly(dT) is too strong to reliably determine binding affinities by fluorescence titrations, we used poly(rU) as a weakly binding substrate (33) to compare the binding strength of *Eco*SSB and *Dra*SSB. Fluorescence titrations at high salt (0.2 M NaCl and 20 mM KP_i) showed no detectable difference in the binding affinity of these proteins (data not shown).

For low salt concentrations (22 mM NaCl), it has been reported that binding of *Eco*SSB to long ssDNA is highly cooperative. At intermediate saturation, such cooperativity

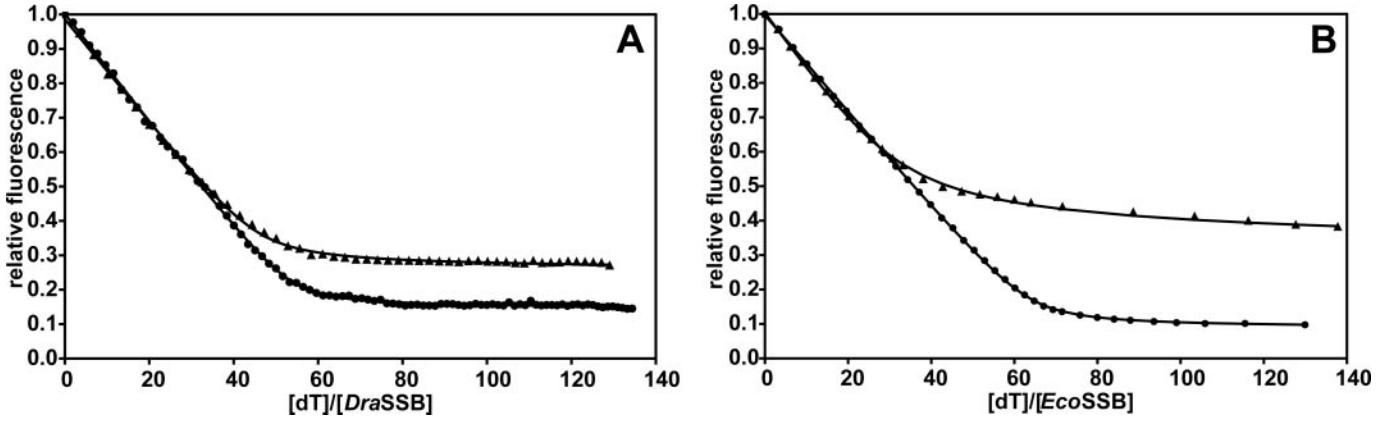

Figure 4. Fluorescence titrations of *Dra*SSB and *Eco*SSB with poly(dT) at 22°C and different salt conditions. Solid lines are theoretical binding isotherms for the binding of a multidentate ligand to a linear polymer (23) with binding site size n and cooperative affinity $\omega \cdot K$ as indicated below. (**A**) Circles: 0.375 µM *Dra*SSB in 0.3 M NaCl, 20 mM KP_i, 100 p.p.m. Tween-20; $n = 53.9$, $\omega \cdot K = 1.2 \times 10^8$ M^{-1}, $Q_f = 86.2\%$. Triangles: 0.375 µM *Dra*SSB in 1 mM NaCl, 1 mM KP_i, 100 p.p.m. Tween-20; $n = 47.5$, $\omega \cdot K = 5 \times 10^7$ M^{-1}, $Q_f = 74.9\%$. (**B**) Circles: 0.29 µM *Eco*SSB in 0.3 M NaCl, 20 mM KP_i, 0.1 mM EDTA, 100 p.p.m. Tween-20; $n = 63.7$, $\omega \cdot K = 1.5 \times 10^8$ M^{-1}, $Q_f = 92\%$. Triangles: 0.44 µM *Eco*SSB in 1 mM NaCl, 1 mM KP_i, 0.1 mM EDTA, 100 p.p.m. Tween-20; $n = 39.5$, $\omega \cdot K = 9.3 \times 10^6$ M^{-1}, $Q_f = 70\%$.

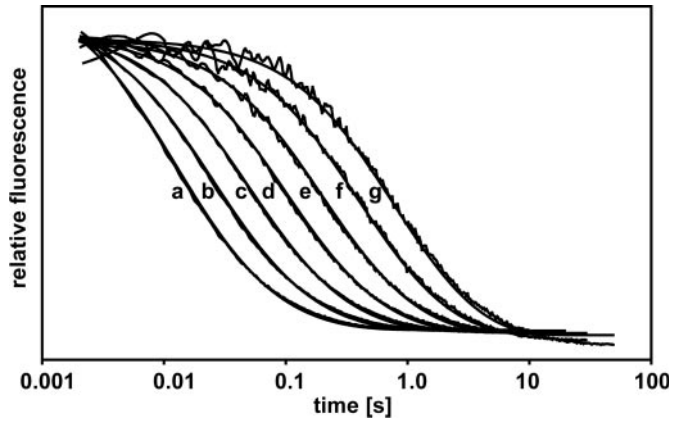

Figure 5. Stopped-flow kinetics of the association of *Dra*SSB with poly(dT) at 0.3 M NaCl, 20 mM KP_i, 100 p.p.m. Tween-20. Concentrations of *Dra*SSB and poly(dT) were (a) 0.8 and 40 μM (b) 0.4 and 20 μM (c) 0.2 and 10 μM (d) 0.1 and 5 μM (e) 50 nM and 2.5 μM (f) 25 nM and 1.25 μM (g) 12.5 nM and 0.625 μM, respectively. The curves were normalized to show equal amplitudes. Smooth lines represent the theoretical time courses for the mechanism described in the text (10) using an association rate constant k_{ass} of 2.1×10^8 M^{-1} s^{-1}, a binding site size *n* of 55 and an initial binding site length of 11 nt.

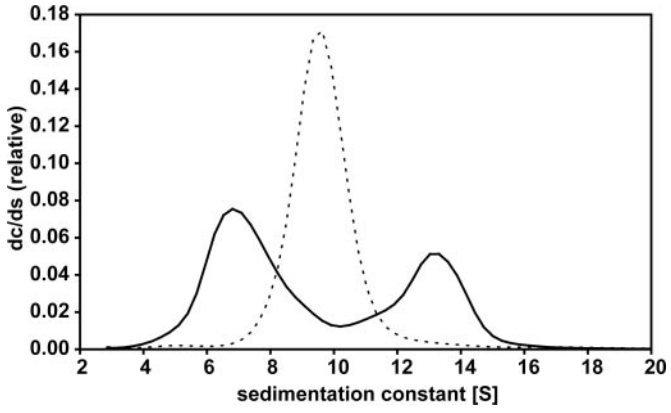

Figure 6. *Dra*SSB shows transient cooperativity by binding to ssDNA at low salt. Mixtures of 0.35 μM *Dra*SSB and 35 μM poly(dT) in 5 mM NaCl, 5 mM KP_i and 0.87 M glycerol were analyzed in sedimentation velocity experiments in the analytical ultracentrifuge (23 000 r.p.m., 20°C, An50Ti rotor) after 1 h (solid line) and 96 h (dotted line) incubation at room temperature. The differential sedimentation coefficient distributions were obtained using the program SEDFIT (19). The initially non-randomly distributed *Dra*SSB molecules redistribute within 96 h on the poly(dT) strands.

leads to a non-random distribution of ssDNA/SSB complexes. Gel electrophoresis of 50% saturated ssM13mp7 DNA showed two different species that were attributed to fully saturated and non-saturated ssDNA (32). Such a bifurcation of SSB distribution on long ssDNA can also be seen in analytical ultracentrifugation experiments with poly(dT) and SSB. In Figure 6, the c(s) distribution (19) of a poly(dT)/*Dra*SSB mixture at low salt conditions (5 mM NaCl, 5 mM KP_i and 0.87 M glycerol) is shown. Sedimenting the mixture shortly (1 h) after preparation leads to two different complexes with ~7S and 13S, respectively. Glycerol had to be added to avoid protein aggregation and owing to its viscosity increment free poly(dT) and *Dra*SSB sediment with 4S and 3S, respectively, in this buffer. The non-random distribution of *Dra*SSB molecules on the poly(dT) strands is a consequence of the highly cooperative binding. If, however, the mixture of *Dra*SSB and poly(dT) is incubated for longer periods (24–96 h), the two species merge and after 4 days incubation at room temperature only a single species sedimenting with an intermediate sedimentation constant (10S) can be detected (Figure 6). Therefore, the *Dra*SSB molecules that initially bind in a non-random distribution redistribute very slowly on the poly(dT) strands. This slow rearrangement reflects a very large lifetime of *Dra*SSB bound cooperatively to poly(dT). For *Eco*SSB under the same buffer conditions, we could also observe non-random distribution on poly(dT) by analytical ultracentrifugation confirming gel electrophoretic experiments reported previously (32). However, redistribution of *Eco*SSB is much slower and even after prolonged incubation (2 weeks), we could not reach fully random distribution (data not shown). Thus, cooperatively bound *Dra*SSB more easily redistributes on poly(dT) than *Eco*SSB.

At high salt conditions (0.3 M NaCl and 20 mM KP_i), both SSB proteins showed a random distribution on the poly(dT) strands independent of incubation time (data not shown). Therefore high DNA-binding cooperativity under high salt conditions could be excluded.

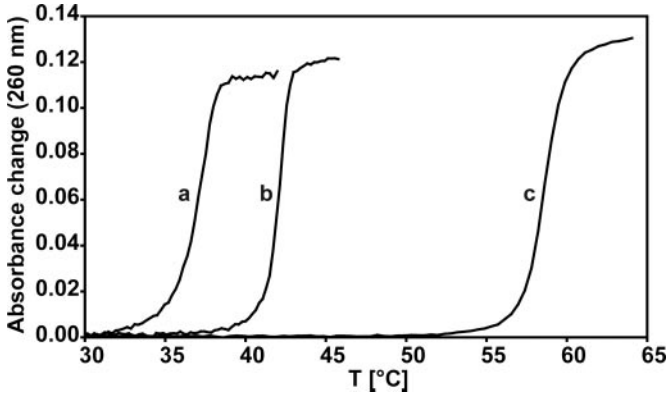

Figure 7. *Dra*SSB and *Eco*SSB show different influence on the melting behavior of poly(dA–dT). Samples containing 38 μM nucleotides of poly(dA–dT) in a buffer containing 75 mM NaCl and 20 mM KP_i were melted in the presence of 3.25 μM *Eco*SSB (a), 3.25 μM *Dra*SSB (b) and in the absence of protein (c).

As a thermodynamic consequence of SSB proteins binding specifically to ssDNA and not to dsDNA, a destabilization of DNA double strands in the presence of SSB must be expected. Figure 7 shows that the melting temperature of poly(dA–dT) is decreased from 59 to 42°C by excess amounts of *Dra*SSB. Under the same conditions, *Eco*SSB decreases the melting temperature from 59 to 37°C, indicating a weaker affinity of *Dra*SSB for ssDNA under the conditions of the melting experiment.

Protein–protein interactions of *Dra*SSB

As described earlier, the C-terminal region of *Eco*SSB is responsible for protein–protein interactions (28–30). Since the corresponding sequences of *Dra*SSB and *Eco*SSB are highly homologous, there is a high possibility of corresponding interactions in *D.radiodurans* (9). One of the proteins functionally interacting with the C-terminus of *Eco*SSB is

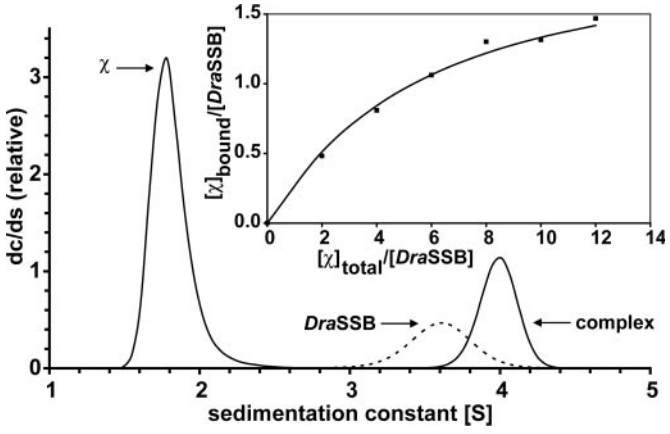

Figure 8. Interaction of *Dra*SSB and *E.coli* DNA polymerase III χ subunit detected by analytical ultracentrifugation. Analytical sedimentation velocity centrifugation of 2.65 μM *Dra*SSB (dotted line) and a mixture of 2.65 μM *Dra*SSB and 31.8 μM χ (solid line) in 0.3 M NaCl, 20 mM KP_i at 20°C and 50 000 r.p.m. Differential sedimentation coefficient distributions were obtained using the program SEDFIT (19). In the presence of χ, a complex is formed which sediments faster than any of the free proteins. Inset: for different mixtures concentrations of free and bound χ were determined from the areas under the separated peaks of the differential sedimentation coefficient distributions and were used to construct a binding isotherm. The solid line represents the best non-linear least squares fit for independent binding of 2.2 χ molecules to a *Dra*SSB dimer with $K = 7.4 \times 10^4$ M^{-1}.

the χ subunit of *E.coli* DNA polymerase III, for which qualitative and quantitative studies of the interaction have been reported previously (29,30). Thus, and since we have shown that *Dra*SSB can take over *Eco*SSB function in *E.coli*, we decided to test protein–protein interactions of *Dra*SSB using χ protein of *E.coli* as a ligand. Figure 8 shows a c(s) distribution (19) of the sedimentation of *Dra*SSB in the presence and absence of χ. Binding of χ leads to an increase of the sedimentation coefficient from 3.6S for free *Dra*SSB to ~4S. A binding isotherm constructed from an analysis of boundary heights shows binding of 2 χ proteins to a *Dra*SSB dimer with an approximate affinity of 10^5 M^{-1} (Figure 8, inset). Therefore, in *Dra*SSB all C-terminal regions are accessible for χ binding.

DISCUSSION

Sequence similarity classifies the ssDNA-binding protein of *D.radiodurans* to belong to the class of homotetrameric SSB proteins. However, the protomer of *Dra*SSB is nearly twice the size of typical homotetrameric SSB protein subunits. Whereas the protomers of the tetrameric SSB proteins contain only one DNA-binding domain (OB-fold), the SSB protein from *D.radiodurans* and from other species of the *Thermus* group contain two OB-folds (7), indicating a gene duplication in the evolution of the *Thermus* group of bacteria.

From *D.radiodurans* cells (strain DSM20539), we amplified the *ssb* gene by PCR. Analysis of the DNA sequence resulted in an ORF coding for 301 amino acids and revealed sequencing errors in the genomic sequence originally published (34). These errors were recently reported by others also (9). After cloning of the *Dra*SSB gene, we expressed the protein in *E.coli* and purified it to homogeneity. By western blot analysis, we could show that recombinant *Dra*SSB protein cross-reacts with anti-*Eco*SSB antibodies and we identified the same protein in a total protein extract of *D.radiodurans*.

Sedimentation equilibrium experiments of *Dra*SSB gave a molar mass of 62 kg/mol, clearly showing that *Dra*SSB forms dimers in solution. This is in excellent agreement with the results of (9). Sedimentation velocity analysis revealed a frictional ratio of 1.5, which indicates that the *Dra*SSB dimer must be either strongly asymmetric or globular with protrusions. *Dra*SSB, like other proteins from the class of homotetrameric SSB proteins, contains in its C-terminal part a proline- and glycine-rich region, which is expected to be very flexible. Therefore, it seems probable that the high frictional ratio of *Dra*SSB, as well as of the other bacterial SSB proteins (11), is caused by the extension of this region into the solution. Similarly to the other homologs, in *Dra*SSB the proline- and glycine-rich region is succeeded by the last 10 amino acids, which are highly conserved in this class. For *Eco*SSB, it could be shown that this region is responsible for the interaction with other proteins involved in DNA metabolism (28–30,35). It has been speculated that the glycine- and proline-rich region acts as a spacer between the DNA-binding domain and the negatively charged region of the last 10 amino acids (36). Thus, the formation of complexes between SSB proteins and their interaction partners could be facilitated by an easy access of this region. We showed that a *Dra*SSB dimer interacts with up to two molecules of *E.coli* DNA polymerase III χ subunit. Having four protomers *Eco*SSB protein binds up to four χ molecules (30). Thus, both C-terminal regions of the dimeric *Dra*SSB are accessible for the interaction with other proteins. The affinity of the *Dra*SSB/χ interaction is $\sim 10^5$ M^{-1}, similar to the affinity of the *Eco*SSB/χ interaction (30), despite the fact that *E.coli* DNA polymerase III χ subunit is not a natural interaction partner of *Dra*SSB *in vivo*. This again demonstrates that interactions of the bacterial SSB proteins with other proteins are evolutionarily conserved and that the conserved region of the last 10 amino acids plays a crucial role in these interactions (36).

It remains to be noted that *in silico* analysis of *D.radiodurans* genome failed to reveal an ORF coding for a protein homologous to the χ subunit of DNA polymerase III from *E.coli*. Other proteins known to interact with bacterial SSB proteins [uracil DNA glycosylase (35) and primase (37)], however, have been identified *in silico* (Q9RWH9, Q9RWR5, respectively). Thus, it seems likely that evolutionary divergence led to a χ protein in *D.radiodurans* that could not be detected by the present *in silico* methods.

*Eco*SSB is essential for the survival of the *E.coli* cell (15), and the conserved region of the last 10 amino acids is necessary for *Eco*SSB functioning *in vivo* (36). Using an *ssb* deletion strain, we could show that *Dra*SSB can take over the function of *Eco*SSB *in vivo*. Since *Dra*SSB as a dimer contains only two instead of four C-termini, two C-termini seem to suffice for the *in vivo* function of SSB. It has been speculated that the loss of two of the four C-termini in *Dra*SSB may lead to functional differences (9). Our data clearly show that such functional differences, even if they exist, do not play an important role in the function of SSB *in vivo*.

The tetrameric human mitochondrial SSB (*Hs*mtSSB) protein cannot complement an *Eco*SSB deletion mutant strain (36), although it is structurally strongly related and shares 32%

sequence homology with *Eco*SSB (4,5). Since the mitochondrial SSB proteins contain no part homologous to the C-terminal region of the bacterial SSB proteins (25), this finding was not unexpected. A chimeric protein composed of the DNA-binding domain of *Hs*mtSSB and the C-terminal third of *Eco*SSB is not able to take over *Eco*SSB function *in vivo* either (36). Therefore, the functional homology of the DNA-binding domains of the tetrameric *Eco*SSB and the dimeric *Dra*SSB must be larger than the functional homology between the homotetrameric proteins *Eco*SSB and *Hs*mtSSB.

We showed that the binding of *Dra*SSB to ssDNA results in a quench of tryptophan fluorescence by >75% under all salt conditions used. Therefore, we used fluorescence titrations for a detailed characterization of the DNA-binding properties of *Dra*SSB. Independent of salt concentration, the binding affinity of *Dra*SSB and poly(dT) is larger than 10^7 M^{-1}. The binding site size of *Dra*SSB is slightly salt dependent and varies between 54 nt per *Dra*SSB dimer at high and 47 nt at low salt concentrations (0.3 M NaCl and 20 mM KP_i, 1 mM NaCl and 1 mM KP_i, respectively). For *Eco*SSB, at least two distinctly different DNA-binding modes have been described (38). Whereas under high salt conditions, 65 nt bind per *Eco*SSB tetramer with almost 90% fluorescence quench, under low salt conditions 35 nt are sufficient to saturate the protein and quench its fluorescence by only 53%. Therefore, comparison of the DNA-binding properties of *Dra*SSB and *Eco*SSB gives a slightly reduced binding site size for *Dra*SSB under high salt conditions. The distinctly different binding mode of *Eco*SSB under low salt conditions could not be observed for *Dra*SSB. Based on the structure of a complex of *Eco*SSB and two molecules of $(dC)_{35}$, a model of the low salt binding mode of *Eco*SSB has been postulated (39). In this model, the Trp54 residues of only two subunits of *Eco*SSB are involved in DNA binding. The most important difference between the structures of *Dra*SSB and *Eco*SSB lies in the fact that *Dra*SSB contains two instead of one DNA-binding domain per monomer. These two binding domains (OB-folds) could evolve separately and amino acids known to be involved in DNA binding were conserved more in the C-terminal OB-fold than in the N-terminal one (7). Therefore, it has been speculated that an asymmetric DNA-binding mode, comparable with the *Eco*SSB low salt mode, is conserved in *Dra*SSB in which only the C-terminal domains are used for DNA binding (7). Our present data do not support such a speculation since they show that under none of the conditions used a distinct binding mode corresponding to the low salt mode of *Eco*SSB could be found. The slight reduction of binding site size at high salt compared with *Eco*SSB is most probably owing to the somewhat smaller overall size of *Dra*SSB. The absence of a low salt binding mode and the fact that *Dra*SSB is functional in *E.coli in vivo* leads us to speculate that the low salt binding mode does not play a vital role in the life of *E.coli*.

Stopped-flow analysis of binding of *Dra*SSB to poly(dT) showed that the association mechanism and rate constant are quite similar to those of the class of the homotetrameric SSB proteins (10,25).

By binding specifically to ssDNA SSB proteins destabilize DNA double strands. Comparison of DNA melting of poly(dA–dT) in the presence of *Dra*SSB and *Eco*SSB respectively, revealed a weaker destabilization of the double strand by *Dra*SSB than by *Eco*SSB. Since in this type of experiment the temperature is varied, differences in ssDNA-binding affinity may also reflect different temperature dependence of protein stability or DNA-binding affinity. Both GuaHCl denaturation experiments in sedimentation equilibrium and irreversible denaturation of *Dra*SSB at temperatures above 50°C in our DNA melting experiments led to the conclusion that *Dra*SSB is less stable than *Eco*SSB. Therefore, we decided to measure the binding affinity at room temperature using poly(rU) as a relatively weak binding substrate. In these experiments, no difference in nucleic acid binding affinity of *Dra*SSB and *Eco*SSB could be detected.

Sedimentation velocity experiments under low salt conditions showed that *Dra*SSB bound to excess poly(dT) shows a highly asymmetric distribution caused by a large cooperativity of binding. These cooperative complexes are not at equilibrium and redistribute after 96 h of incubation. Such a formation of transiently highly cooperative complexes has also been described for *Eco*SSB (32). However, the redistribution of the non-randomly bound SSB proteins is much faster in the case of *Dra*SSB.

In summary, our observations let *Dra*SSB seem to be a normal representative of bacterial SSB proteins. Except for the absence of a low salt binding mode, *Dra*SSB has all the essential properties of the prototype *Eco*SSB, including the ability to take over the vital role of *Eco*SSB in *E.coli* cells. The question as to why evolution chose to create homodimeric bacterial SSB proteins remains open.

ACKNOWLEDGEMENTS

We thank Lidia Litz for expert technical assistance and Dr Joachim Greipel for valuable discussions. Funding to pay the Open Access publication charges for this article was provided by the Medical School Hannover.

Conflict of interest statement. None declared.

REFERENCES

1. Murzin,A.G. (1993) OB(oligonucleotide/oligosaccharide binding)-fold: common structural and functional solution for non-homologous sequences. *EMBO J.*, **12**, 861–867.
2. Suck,D. (1997) Common fold, common function, common origin? *Nature Struct. Biol.*, **4**, 161–165.
3. Raghunathan,S., Ricard,C.S., Lohman,T.M. and Waksman,G. (1997) Crystal structure of the homo-tetrameric DNA binding domain of *Escherichia coli* single-stranded DNA-binding protein determined by multiwavelength X-ray diffraction on the selenomethionyl protein at 2.9-Å resolution. *Proc. Natl Acad. Sci. USA*, **94**, 6652–6657.
4. Webster,G., Genschel,J., Curth,U., Urbanke,C., Kang,C.H. and Hilgenfeld,R. (1997) A common core for binding single-stranded DNA: structural comparison of the single-stranded DNA-binding proteins (SSB) from *E.coli* and human mitochondria. *FEBS Lett.*, **411**, 313–316.
5. Yang,C., Curth,U., Urbanke,C. and Kang,C. (1997) Crystal structure of human mitochondrial single-stranded DNA binding protein at 2.4 Å resolution. *Nature Struct. Biol.*, **4**, 153–157.
6. Dabrowski,S., Olszewski,M., Piatek,R. and Kur,J. (2002) Novel thermostable ssDNA-binding proteins from *Thermus thermophilus* and *T.aquaticus*-expression and purification. *Protein Expr. Purif.*, **26**, 131–138.
7. Bernstein,D.A., Eggington,J.M., Killoran,M.P., Misic,A.M., Cox,M.M. and Keck,J.L. (2004) Crystal structure of the *Deinococcus radiodurans* single-stranded DNA-binding protein suggests a mechanism for coping with DNA damage. *Proc. Natl Acad. Sci. USA*, **101**, 8575–8580.

8. Dabrowski,S., Olszewski,M., Piatek,R., Brillowska-Dabrowska,A., Konopa,G. and Kur,J. (2002) Identification and characterization of single-stranded-DNA-binding proteins from *Thermus thermophilus* and *Thermus aquaticus*—new arrangement of binding domains. *Microbiology*, **148**, 3307–3315.
9. Eggington,J.M., Haruta,N., Wood,E.A. and Cox,M.M. (2004) The single-stranded DNA-binding protein of *Deinococcus radiodurans*. *BMC Microbiol.*, **4**, 2.
10. Urbanke,C. and Schaper,A. (1990) Kinetics of binding of single-stranded DNA binding protein from *Escherichia coli* to single-stranded nucleic acids. *Biochemistry*, **29**, 1744–1749.
11. Williams,K.R., Spicer,E.K., Lopresti,M.B., Gugenheimer,R.A. and Chase,J.W. (1983) Limited proteolysis studies on the *E.coli* single-stranded DNA binding protein. *J. Biol. Chem.*, **258**, 3346–3355.
12. Gill,S.C. and von Hippel,P.H. (1989) Calculation of protein extinction coefficients from amino acid sequence data. *Anal. Biochem.*, **182**, 319–326.
13. Böhme,H.J., Kopperschlägel,G., Schulz,J. and Hofmann,E. (1972) Affinity chromatography of phosphofructokinase using cibachrome blue F36-A. *J. Chromatogr.*, **69**, 209–214.
14. Laemmli,U.K. (1970) Cleavage of structural proteins during the assembly of the head of bacteriophage T4. *Nature*, **227**, 680–685.
15. Porter,R.D., Black,S., Pannuri,S. and Carlson,A. (1990) Use of the *Escherichia coli ssb* gene to prevent bioreactor takeover by plasmidless cells. *Biotechnology*, **8**, 47–51.
16. Bayer,I., Fliess,A., Greipel,J., Urbanke,C. and Maass,G. (1989) Modulation of the affinity of the single-stranded DNA-binding protein of *Escherichia coli* (*E.coli* SSB) to poly(dT) by site-directed mutagenesis. *Eur. J. Biochem.*, **179**, 399–404.
17. Lamm,O. (1929) Die Differentialgleichung der Ultrazentrifugierung. *Arkiv Matematik Astronomi Fysik*, **21B**, 1–4.
18. Kindler,B. (1997) AKKUPROG: Auswertung von Messungen chemischer Reaktionsgeschwindigkeit und Analyse von Biopolymeren in der Ultrazentrifuge. Anwendung auf Protein-DNA Wechselwirkungen. PhD Thesis, Universität Hannover, Hannover, Germany.
19. Schuck,P. (2000) Size-distribution analysis of macromolecules by sedimentation velocity ultracentrifugation and Lamm equation modeling. *Biophys. J.*, **78**, 1606–1619.
20. Urbanke,C., Witte,G. and Curth,U. (2005) A sedimentation velocity method in the analytical ultracentrifuge for the study of protein–protein interactions. In Nienhaus,G.U. (ed.), *Protein-Ligand Interactions: Methods and Applications*. Humana Press, Totowa, NJ, Vol. 305, pp. 101–114.
21. Durchschlag,H. (1986) Specific volumes of biological macromolecules and some other molecules of biological interest. In Hinz,H. (ed.), *Thermodynamic Data for Biochemistry and Biotechnology*. Springer, Berlin, Heidelberg, pp. 45–128.
22. Augustyns,K., Van Aerschot,A., Van Schepdael,A., Urbanke,C. and Herdewijn,P. (1991) Influence of the incorporation of (S)-9-(3,4-dihydroxybutyl)adenine on the enzymatic stability and base-pairing properties of oligodeoxynucleotides. *Nucleic Acids Res.*, **19**, 2587–2593.
23. Curth,U., Greipel,J., Urbanke,C. and Maass,G. (1993) Multiple binding modes of the single-stranded DNA binding protein from *Escherichia coli* as detected by tryptophan fluorescence and site-directed mutagenesis. *Biochemistry*, **32**, 2585–2591.
24. Schwarz,G. and Watanabe,F. (1983) Thermodynamics and kinetics of co-operative protein-nucleic acid binding. I. General aspects of analysis of data. *J. Mol. Biol.*, **163**, 467–484.
25. Curth,U., Urbanke,C., Greipel,J., Gerberding,H., Tiranti,V. and Zeviani,M. (1994) Single-stranded-DNA-binding proteins from human mitochondria and *Escherichia coli* have analogous physicochemical properties. *Eur. J. Biochem.*, **221**, 435–443.
26. Sancar,A., Williams,K.R., Chase,J.W. and Rupp,W.D. (1981) Sequences of the *ssb* gene and protein. *Proc. Natl Acad. Sci. USA*, **78**, 4274–4278.
27. Lebowitz,J., Lewis,M.S. and Schuck,P. (2002) Modern analytical ultracentrifugation in protein science: a tutorial review. *Protein Sci.*, **11**, 2067–2079.
28. Genschel,J., Curth,U. and Urbanke,C. (2000) Interaction of *E.coli* single-stranded DNA binding protein (SSB) with exonuclease I. The carboxy-terminus of SSB is the recognition site for the nuclease. *Biol. Chem.*, **381**, 183–192.
29. Kelman,Z., Yuzhakov,A., Andjelkovic,J. and O'Donnell,M. (1998) Devoted to the lagging strand-the χ subunit of DNA polymerase III holoenzyme contacts SSB to promote processive elongation and sliding clamp assembly. *EMBO J.*, **17**, 2436–2449.
30. Witte,G., Urbanke,C. and Curth,U. (2003) DNA polymerase III χ subunit ties single-stranded DNA binding protein to the bacterial replication machinery. *Nucleic Acids Res.*, **31**, 4434–4440.
31. DeVries,J., Genschel,J., Urbanke,C., Thole,H. and Wackernagel,W. (1994) The single-stranded-DNA-binding proteins (SSB) of *Proteus mirabilis* and *Serratia marcescens*. *Eur. J. Biochem.*, **224**, 613–622.
32. Lohman,T.M., Overman,L.B. and Datta,S. (1986) Salt-dependent changes in the DNA binding co-operativity of *Escherichia coli* single strand binding protein. *J. Mol. Biol.*, **187**, 603–615.
33. Bujalowski,W. and Lohman,T.M. (1987) A general method of analysis of ligand-macromolecule equilibria using a spectroscopic signal from the ligand to monitor binding. Application to *Escherichia coli* single-strand binding protein–nucleic acid interactions. *Biochemistry*, **26**, 3099–3106.
34. White,O., Eisen,J.A., Heidelberg,J.F., Hickey,E.K., Peterson,J.D., Dodson,R.J., Haft,D.H., Gwinn,M.L., Nelson,W.C., Richardson,D.L. *et al.* (1999) Genome sequence of the radioresistant bacterium *Deinococcus radiodurans* R1. *Science*, **286**, 1571–1577.
35. Handa,P., Acharya,N. and Varshney,U. (2001) Chimeras between single-stranded DNA-binding proteins from *Escherichia coli* and *Mycobacterium tuberculosis* reveal that their C-terminal domains interact with uracil DNA glycosylases. *J. Biol. Chem.*, **276**, 16992–16997.
36. Curth,U., Genschel,J., Urbanke,C. and Greipel,J. (1996) *In vitro* and *in vivo* function of the C-terminus of *Escherichia coli* single-stranded DNA binding protein. *Nucleic Acids Res.*, **24**, 2706–2711.
37. Yuzhakov,A., Kelman,Z. and O'Donnell,M. (1999) Trading places on DNA-a three-point switch underlies primer handoff from primase to the replicative DNA polymerase. *Cell*, **96**, 153–163.
38. Lohman,T.M. and Bujalowski,W. (1990) *E.coli* single strand binding protein: multiple single stranded DNA binding modes and cooperativities. In Revzin,A. (ed.), *The Biology of Non Specific Protein DNA Interactions*. CRC Press, Boca Raton, FL, pp. 131–168.
39. Raghunathan,S., Kozlov,A.G., Lohman,T.M. and Waksman,G. (2000) Structure of the DNA binding domain of *E.coli* SSB bound to ssDNA. *Nature Struct. Biol.*, **7**, 648–652.
40. Schägger,H. and Jagow,G. (1987) Tricine–sodium dodecyl sulfate–polyacrylamide gel electrophoreis for the separation of proteins in the range from 1 to 100 kDa. *Anal. Biochem.*, **166**, 368–379.